Nonlinear hydrodynamics of a hard-sphere fluid near the glass transition

Lisa M. Lust and Oriol T. Valls
School of Physics and Astronomy and Minnesota Supercomputer Institute, University of Minnesota, Minneapolis, Minnesota 55455-0149

Chandan Dasgupta
Department of Physics, Indian Institute of Science, Bangalore 560012, India
(Received 1 December 1992)

We conduct a numerical study of the dynamic behavior of a dense hard-sphere fluid by deriving and integrating a set of Langevin equations. The statics of the system is described by a free-energy functional of the Ramakrishnan-Yussouff form. We find that the system exhibits glassy behavior as evidenced through a stretched exponential decay and a two-stage relaxation of the density correlation function. The characteristic times grow with increasing density according to the Vogel-Fulcher law. The wave-number dependence of the kinetics is extensively explored. The connection of our results with experiment, mode-coupling theory, and molecular-dynamics results is discussed.

PACS number(s): 61.20.Ja, 64.70.Pf, 61.20.Lc, 02.60.−x

I. INTRODUCTION

Despite extensive experimental, numerical, and theoretical investigations [1,2] over several decades, the present understanding of the slow nonexponential dynamics of dense liquids near the glass transition remains incomplete. When a liquid is cooled rapidly enough to temperatures below the equilibrium freezing temperature, crystallization is bypassed and the system undergoes a transition into an amorphous solid state called a glass. The characteristic relaxation time t^*, as reflected in a large number of experimentally measured quantities such as viscosity and dielectric relaxation, grows rapidly in the supercooled state as the temperature is decreased or the density increased. The glass-transition temperature (or alternatively, density) T_g (ρ_g) is conventionally defined as the temperature (density) where the viscosity reaches a value of 10^{13} P.

In recent years, considerable progress in the development of a theoretical and experimental understanding of the phenomena associated with glass formation and the glass transition has been achieved. In particular, the so-called mode-coupling (MC) theories of the glass transition [3–10] have led to a framework for understanding and interpreting many experimental results. In MC theories, the slowing down of the dynamics near the glass transition is attributed to a nonlinear feedback mechanism arising from correlations of density fluctuations in the liquid. The MC equations for the dynamics near the glass transition were originally derived [4,5] from the kinetic theory of dense fluids and were later generalized and extended by Götze and co-workers [6,7]. In the original version of MC theories [4,5], the characteristic time scales of the liquid are predicted to exhibit a power-law divergence at an "ideal glass transition" or crossover temperature T_c, higher than T_g. However, this divergence is not found experimentally: the power-law form breaks down, and relaxation times at T_c are typically of order 10^{-8} s. More recent calculations [9,10] have uncovered a cutoff mechanism which is supposed to round off the predicted divergence and restore ergodicity over a much longer time scale. Most of the existing MC studies of the glass transition do not take into account the equilibrium short-range structure of the dense liquid. As a result, these theories do not lead to any prediction for the wave-number dependence of the relaxation. Some attempts towards the incorporation of information about liquid structure in the MC formalism have been made recently [8,10]. MC theories [3,7] and experimental information can be combined in a consistent description of the decay of $S(\mathbf{q},t)$, the spatial Fourier transform of the dynamic density correlation function, at sufficiently low temperatures or high densities, when the decay times have grown very large. The decay according to this scheme takes place in a succession of several regimes: after a fast decay in times of order of the inverse phonon frequency, a first slow decay occurs which MC theories predict to be an inverse power law in time. This is called the β-relaxation regime. Evidence for power-law decay of correlations in the β regime is provided by light- and neutron-scattering experiments [12]. This decay is to a nonzero value (an apparent nonergodic phase) from which the system eventually moves away leading to the primary or α-relaxation regime. The relaxation in the α regime is found to follow the so-called Kohlrausch-Williams-Watts "stretched exponential" form [13]. Both the duration of the β relaxation and the time scale of the stretched exponential decay in the α regime are found to increase sharply as the "glass transition" is approached. In some cases, the β and the α regimes are separated by a region of so-called von Schweidler relaxation which has a power-law form. The stretched exponential behavior in the α regime and the von Schweidler relaxation are seen in dielectric measurements [14] and in light- [15] and neutron-scattering [16] experiments. The parameters which describe the decay of $S(\mathbf{q},t)$ are known to be q

dependent, but the nature of this dependence has not been studied in detail. Thus, the MC theories provide a qualitative understanding of a number of experimentally observed features of glassy relaxation. However, some of the detailed MC predictions are not in agreement with experiments [17] and the MC description clearly fails to account for the behavior observed at temperatures close to and lower than T_c. It is generally believed [3] that this failure arises from the fact that MC theories do not take into account activated processes involving transitions between different local minima of the free energy which are supposed to develop as the temperature is lowered below the equilibrium freezing temperature.

In contrast to MC theories which portray the glass transition as being purely dynamic in nature, there have been a number of attempts [18–21] to develop a "thermodynamic" theory in which some of the interesting behavior observed near the glass transition is attributed to an underlying continuous phase transition. These attempts have been motivated by the fact that the observed growth of the relaxation time in so-called "fragile" liquids [2] is well described by the Vogel-Fulcher law [22]:

$$t^* = \tau_s e^{aT_0/(T-T_0)} , \tag{1.1}$$

where τ_s is a characteristic microscopic time, a is a dimensionless constant, and T_0 is a characteristic temperature which is found to be well below the conventional glass-transition temperature T_g. This law suggests the possibility of a so-called "thermodynamic glass transition" that would take place at the temperature T_0 if thermodynamic equilibrium [23] could be maintained down to this temperature. Such a transition is also suggested by the fact [2] that the Kauzmann temperature [24] at which the entropy difference between the supercooled liquid and the crystalline solid extrapolates to zero is close to T_0. Since in practice the system falls out of equilibrium at temperatures close to T_g, a direct experimental test of the existence of such a transition is not possible. Also, any calculation that explicitly demonstrates the existence of such a transition in a physically realistic system is not yet available. Thus, the thermodynamic-glass-transition scenario remains essentially speculative. In this approach, the growth of the relaxation time is attributed to a growing correlation length which would diverge at the ideal glass transition. Two recent numerical studies [25,26] which looked for such a growing correlation length did not find any evidence for its existence. A recent experiment [27], on the other hand, has presented evidence for the existence of a length scale that grows as the temperature is lowered below the crossover temperature T_c.

The static and dynamic properties of dense liquids have also been studied extensively by molecular-dynamics (MD) simulations [28–32]. The very nature of the simulation method restricts such studies to simple model systems and to time scales which are rather short (of the order of 10^{-9} s). In spite of these limitations, MD simulations have produced a number of interesting results which are in qualitative agreement with predictions of MC theories and results of experiments (such as those using the neutron spin-echo technique [33]) which have time scales comparable to those of the simulations. This observation leads to the interesting and useful conclusion that a study of simple model systems may be sufficient for understanding the basic physics of the glass transition.

It is evident from this brief survey of the current status of the glass-transition problem that an obvious need exists for the development of new analytic and numerical methods which may address some of the outstanding issues related to this problem. In this paper we describe the results obtained from the application of a new numerical method to a study of the dynamic behavior of a dense hard-sphere liquid near the glass transition. The method we use consists of direct numerical integration of a set of Langevin equations which describe the nonlinear fluctuating hydrodynamics [34] (NFH) of the system. Information about the static structure of the liquid is incorporated in the Langevin equations through a free-energy functional which has a form suggested by Ramakrishnan and Yussouff [35] (RY). Recently, it has been shown [36] that the RY free-energy functional provides a correct mean-field description of the statics of the glass transition in this system. In that work a numerical procedure was used to locate local minima of a discretized version of the RY free energy appropriate for the hard-sphere system. A large number of glassy local minima with inhomogeneous but aperiodic density distribution were found to appear as the average density was increased above the value at which equilibrium crystallization takes place. At higher densities, the free energies of these minima were found to drop below that of the minimum representing the uniform liquid, signaling a mean-field glass transition. The success of the RY free-energy functional in providing a correct description of the statics of the glass transition of the hard-sphere system suggests that a good starting point for a study of the dynamics of this system would be obtained by incorporating this free energy in the appropriate NFH equations.

A number of important issues are addressed in our study of the dynamics. By comparing the results of our calculations with existing MD results [28] on the same system, we are able to test the validity of the NFH description which is cast in terms of coarse-grained number and current density variables instead of the coordinates and momenta of individual particles. The correctness of the NFH equations we use, although usually taken for granted, it not obvious in view of the fact that the hydrodynamic terms in these equations describe the physics at relatively long length scales, whereas the terms arising from the free-energy functional involve length scales of the order of (or smaller than) the interparticle spacing. In the RY free-energy functional, information about the microscopic interactions is incorporated in the form of the Ornstein-Zernike direct pair-correlation function [37] of the liquid. This appears to be adequate for a correct description of the statics of the freezing of the liquid into both crystalline [35] and glassy [36] states. One of the questions we address in the present study is whether this is also sufficient for a correct description of the dynamic behavior. Two numerical studies of NFH

equations describing the dynamics of dense liquids have been reported recently [38,39]. The main difference between these studies and the present one is that the equilibrium structure of the liquid was treated only in an approximate way in the earlier calculations. Consequently, the results of these calculations could not be compared directly with MD data. The results of these calculations did not exhibit some of the features (such as two-regime decay of correlations) generally associated with glassy dynamics, although nonexponential decay of correlations often associated with its onset was found. In Ref. [39] it was suggested that this failure arises from the approximations made in the treatment of liquid structure. The present study provides the opportunity to check whether this explanation is correct and to investigate in general the role of static structure in the dynamics of a dense liquid. Further, perturbative treatments of the NFH equations similar to the ones we use are known [9,10] to lead to results which are very close to those obtained from the MC approach. Apart from numerical errors arising from spatial discretization and the integration procedure, our treatment of these equations is exact. In particular, our numerical solution of these equations is obviously nonperturbative; therefore, a comparison of the results of our calculation with MC predictions provides a way to test the validity of some of the approximations made in the analytic studies. Since our calculation takes full account of the short-range structure of the liquid, it has the most direct connection with the MC studies of Kirkpatrick [8] and Das [10]. Finally, by monitoring which minima of the free energy are visited during the time evolution of the system, we are able to determine whether the observed dynamic behavior arises from nonlinearities of density fluctuations in the liquid or from transitions among different glassy minima of the free energy. It is not possible to distinguish between the effects of these two kinds of processes in conventional MD simulations.

We have studied the time decay of $S(q,t)$, the spherically averaged spatial Fourier transform of the time-dependent density correlation function of the hard-sphere liquid, for different values of wave vector q and for a number of values of the reduced density n^* ($n^* \equiv \rho_0 \sigma^3$, where ρ_0 is the average number density and σ is the hard-sphere diameter) in the range 0.75–0.93. It was found in Ref. [36] that a hard-sphere system described by a discretized version of the RY free energy exhibits a crystallization transition near $n^*=0.83$. Since the present calculation uses the same discretized free energy as that of Ref. [36], the system may be considered to be in the "supercooled" regime for a large part of the density range considered by us. The numerical efficiency of the Langevin dynamics arising from the use of coarse-grained variables enables us to verify that the statics of the system remain stationary throughout the long time intervals that we consider. The observed dynamic behavior described later in detail exhibits a number of characteristic glassy features. These include stretched exponential decay of correlations, two-stage relaxation, and Vogel-Fulcher growth of relaxation times. Our results are in agreement with existing MD data [28] on the dynamics of the hard-sphere liquid and in qualitative agreement with other MD results obtained for similar but different systems. This observation establishes the correctness of the NFH description used in this work and also demonstrates that the RY free energy contains the essential physics of the dynamics of this system. Our calculations also reproduce qualitatively a number of predictions of MC theories; however, we find significant deviations from some of the quantitative MC predictions [40] for the glassy kinetics of the hard-sphere system. Our study indicates that the onset of glassy features in the decay of $S(q,t)$ occurs at relatively lower densities for wave vectors close to the first and second peaks in the static structure factor. This result clearly illustrates the important role played by the equilibrium structure in the long-time dynamics of the liquid. The observed q dependence of the decay of $S(q,t)$ also suggests that the glassy behavior sets in earlier (at lower densities) at shorter length scales. Finally, the system is found to fluctuate about the liquid-state minimum of the mean-field free energy in all our simulations.

The rest of the paper is organized as follows: Section II contains a description of the model considered by us. We first define the model, discuss its statics, and derive the appropriate NFH equations. By defining appropriate units of length, time, and mass, these equations are then written in dimensionless form. The method used by us to integrate these equations forward in time is described in Sec. III. We also discuss in this section the physical quantities measured, the data collection procedure, tests of equilibration, and other related matters. The results obtained from the numerical work are described in detail in Sec. IV. We also compare and contrast our results with those obtained from MD simulations of the hard-sphere and similar systems and the predictions of MC theories.

II. THE MODEL

We have explained in the Introduction that we will analyze the numerical solution of a set of Langevin equations appropriate to a dense hard-sphere fluid. We begin here by discussing the statics of the model. These are given in terms of a free energy which is a functional of the two fields in the problem: the density field $\rho(\mathbf{r},t)$ and the current field $\mathbf{g}(\mathbf{r},t)$. This free energy has two terms:

$$F_{\rm tot}[\rho,\mathbf{g}]=(m_0/2)\int d\mathbf{r}\frac{g^2}{\rho_0}+F[\rho]\ , \tag{2.1}$$

where $F[\rho]$ is of the RY form [35]

$$F[\rho]=F_l[\rho_0]+k_BT\left[\int d\mathbf{r}[\rho\ln(\rho/\rho_0)-\delta\rho] -\tfrac{1}{2}\int d\mathbf{r}\,d\mathbf{r}'C(\mathbf{r}-\mathbf{r}')\delta\rho\delta\rho'\right]\ . \tag{2.2}$$

In (2.1) and (2.2), ρ is the number density field and $\delta\rho\equiv\rho-\rho_0$ is the deviation of that field from its average value ρ_0. F_l is the free energy of the uniform liquid, T is the temperature, and k_B the Boltzmann constant. In the first equation, m_0 denotes the mass of a hard sphere. Finally, $C(\mathbf{r}-\mathbf{r}')$ is the direct correlation function. The in-

clusion of this function in the free energy ensures that upon linearization of the logarithm in the first term on the right-hand side of (2.2), one obtains the usual expression for the static structure factor of a simple fluid in terms of C. For hard spheres a simple expression for $C(\mathbf{r}-\mathbf{r}')$ can be obtained in the Percus-Yevick (PY) approximation [37]:

$$C(\xi)=\begin{cases}-\lambda_1-6\eta_f\lambda_2\xi-\frac{1}{2}\eta_f\lambda_1\xi^2, & \xi<1 \quad (2.3a)\\ 0, & \xi>1 \quad (2.3b)\end{cases}$$

where $\xi\equiv|\mathbf{r}-\mathbf{r}'|/\sigma$, η_f is the packing fraction

$$\eta_f=(\pi/6)\rho_0\sigma^3\equiv(\pi/6)n^* , \tag{2.4}$$

and

$$\lambda_1=(1+2\eta_f)^2/(1-\eta_f)^4 , \tag{2.5}$$

$$\lambda_2=-(1+\eta_f/2)^2/(1-\eta_f)^4 . \tag{2.6}$$

We have written ρ_0 in the denominator of the g^2 term in Eq. (2.1), rather than ρ as in Ref. [39], so that the full density dependence of the free energy is given by the RY form. As pointed out in Ref. [41], if we used ρ, we would obtain, upon functional integration with respect to the Gaussian variable g^2, a $\ln(\rho)$ contribution involving density fluctuations associated with the kinetic energy. These are already included in Eq. (2.2).

It is convenient to choose units at this point which will simplify subsequent expressions. We take m_0 as the unit of mass. We choose also a unit of length h, which we shall later identify with the lattice constant of the computational lattice. For the unit of time we choose t_0 such that

$$t_0=h/c , \tag{2.7}$$

where c is the speed of sound. This choice of the unit of time is motivated as follows: The characteristic phonon time for the system is $t_p=1/(cq)$, where q is a wave vector. Hence, $t_p/t_0=1/(qh)$. We shall choose below the ratio σ/h so that qh is of order unity in the wave-vector range of interest. Hence, the choice (2.7) corresponds to a characteristic time of order t_p. The same choice was made in Ref. [39].

We then define the dimensionless quantities

$$\mathbf{x}=\mathbf{r}/h , \tag{2.8}$$

$$n=\rho h^3 , \tag{2.9}$$

$$\mathbf{j}=\mathbf{g}h^3/c \tag{2.10}$$

and introduce also the dimensionless free energy $F[n,\mathbf{j}]$ in terms of the above quantities:

$$F[n,\mathbf{j}]=\tfrac{1}{2}\int d\mathbf{x}\frac{j^2}{n_0}+F_n[n] , \tag{2.11}$$

$$F_n[n]=F_{ln}[n_0]+K\left[\int d\mathbf{x}[n\ln(n/n_0)-\delta n]-\tfrac{1}{2}\int d\mathbf{x}\,d\mathbf{x}'C(\mathbf{x}-\mathbf{x}')\delta n\,\delta n'\right] , \tag{2.12}$$

where

$$K=\frac{k_BT}{m_0c^2} . \tag{2.13}$$

The quantity K is for hard spheres a function of only the density. This follows from

$$c^2=\frac{1}{m_0\rho_0\kappa} , \tag{2.14}$$

where the compressibility κ is related to the structure factor $S(\mathbf{q})$ by $k_BT\rho_0\kappa=S(\mathbf{q}=0)$. The latter quantity can be calculated straightforwardly from (2.3) and one obtains

$$K=\{1+(4\pi/3)n^*[\lambda_1+\tfrac{9}{2}\eta_f\lambda_2+(\eta_f/4)\lambda_1]\}^{-1} , \tag{2.15}$$

which indeed depends on the density only. The quantities λ_1, λ_2, η_f, and n^* were defined above.

We quote here the relation between our unit of time t_0 and the Enskog mean collision time t_c commonly used in MC work [42] on hard spheres. One easily finds that

$$t_c^{-1}=4\sqrt{\pi}n^*g(\sigma)\sqrt{K}\,(h/\sigma)t_0^{-1} , \tag{2.16}$$

where $g(\sigma)$ is the pair-correlation function at contact [43]. The static properties of a system described by the RY free energy, and its relation to glassy behavior, have been discussed in the literature [36,35] and in the Introduction. We turn now to the dynamics. The hydrodynamic variables are, of course, the fields n and $\mathbf{j}$. We denote, following the usual notation, this set of Langevin variables as

$$\{\psi_\alpha\}\equiv\{n(\mathbf{x},t),\mathbf{j}(\mathbf{x},t)\} .$$

Formally, the Langevin equations can be written as [9,44]

$$\frac{\partial\psi_\alpha}{\partial t}=V_\alpha[\psi]-\sum_\beta\Gamma_{\alpha,\beta}\frac{\delta F}{\delta\psi_\beta}+\Theta_\alpha , \tag{2.17}$$

where Γ is the matrix of transport coefficients, Θ are the Gaussian noise fields, and the V_α are the streaming velocities, which incorporate the nondissipative part of the equations of motion. Proceeding as in Refs. [9] and [44], one obtains

$$V_n=-\sum_j\nabla_j\left[n(\mathbf{x})\frac{\delta F}{\delta j_j(\mathbf{x})}\right] , \tag{2.18}$$

$$V_{j_i}=-n(\mathbf{x})\nabla_i\frac{\delta F_n}{\delta n(\mathbf{x})}-\sum_j\nabla_j\frac{j_i(\mathbf{x})j_j(\mathbf{x})}{\mathbf{n}_0}-\sum_j j_j(\mathbf{x})\nabla_i\frac{j_j(\mathbf{x})}{n_0} , \tag{2.19}$$

where F and F_n are defined in Eqs. (2.11) and (2.12). Following then precisely as in Ref. [39], we obtain after straightforward algebra the equations of motion

$$\frac{\partial n(\mathbf{x},t)}{\partial t}+(1/n_0)\nabla(n\mathbf{j})=0 \tag{2.20}$$

and

$$\frac{\partial j_i}{\partial t}=-n\nabla_i\frac{\delta F_n}{\delta n}-(1/n_0)\sum_j\nabla_j(j_ij_j) -(1/n_0)\sum_j j_j\nabla_i j_j+(1/n_0)\eta\nabla^2 j_i+\Theta_i\ , \tag{2.21}$$

where η is the bare shear viscosity in our units [45]. The noise fields $\Theta_i(\mathbf{x},t)$ satisfy the second fluctuation-dissipation theorem in the form

$$\langle\Theta_i(\mathbf{x},t)\Theta_j(\mathbf{x}',t')\rangle=-2K\lambda\eta n_0\delta_{i,j}\nabla^2\delta(\mathbf{r}-\mathbf{r}')\delta(t-t')\ . \tag{2.22}$$

We recall that in these equations, and in the remainder of the paper, the time is measured in units as given in (2.16). In (2.22) the angular brackets denote the thermodynamic average. The quantity λ is a dimensionless measure of the equilibrium fluctuations. The average value n_0 is related to $n^*=n\sigma^3$ through $n_0=n^*(h/\sigma)^3$. For hard spheres [46] one can write η in terms of K and the density in the form

$$\eta=(h/\sigma)^2\sqrt{K}\,[5/(16\sqrt{\pi})][g(\sigma)^{-1}+0.8(2\pi n^*/3) +0.761(2\pi n^*/3)^2 g(\sigma)]\ . \tag{2.23}$$

The equations of motion (2.20) and (2.21) are slightly more complicated than the corresponding equations for the model in Ref. [39]. There is an additional convection term in the second equation and some additional factors of n/n_0. These complications can be directly traced down to the different density dependence of the first term in (2.11) as discussed above, that is, to the fact that a kinetic-energy contribution is now included in the first term of F_n. These differences then arise because of the different form of $\delta F/\delta\mathbf{j}$ which results in more complicated expressions for the streaming velocities. Our expressions correctly reduce to the continuity and Navier-Stokes equations in the linear limit. In general, one can interpret (2.20) as the continuity equation if the field $\mathbf{g}$ is thought of as ρ_0 times the velocity. The current density is then not given simply by $\mathbf{g}$, however. These questions do not affect, obviously, the validity of the conclusions obtained from this model.

A salient feature of Eq. (2.21) which is of considerable importance is that the term in $\delta F_n/\delta n$ which involves the direct correlation function C is an integral over space with range σ. Thus, we have to solve in this case not merely a set of partial differential equations with stochastic terms but, as far as the spatial dependence is concerned, an integro-differential equation. This complication makes this a difficult problem to solve numerically. The methods used will be explained below.

III. METHODS

In this section we discuss the methods we use to solve our equations of motion, the physical quantities we focus on, the data-collection methods and statistics, the range of parameter values we have studied and related matters.

Our objective is to study the dynamic correlations of our system as defined below. In order to do so, we solve numerically Eqs. (2.20) and (2.21) on a three-dimensional cubic lattice of size N^3. The main complication we must consider is the spatial integral involving the direct correlation function $C(\mathbf{r})$. For each integration step this integral must be done N^3 times since it is computed over a sphere with its origin at each one of the lattice sites. To avoid repeated calculations, we create, in the initialization of our program, a table listing for each lattice site the location of all neighboring sites to be integrated over and their correspond values of $C(r)$. Additionally, since the sphere is imbedded on a coarse discrete lattice, we use a finer mesh than defined on the original lattice to improve the accuracy of the integration. The procedures employed to integrate the remaining set of differential equations over time and generate the Gaussian noise are identical to those used in Ref. [39] and references cited therein.

We will focus our analysis on the time dependence of the dynamic structure factor $S(\mathbf{q},t)$:

$$S(\mathbf{q},t)=\int d^3x\, e^{i\mathbf{q}\cdot(\mathbf{x}-\mathbf{x}')}\langle\delta n(\mathbf{x},0)\delta n(\mathbf{x}',t)\rangle\ . \tag{3.1}$$

Specifically, we will consider the angular average of $S(\mathbf{q},t)$. On a cubic lattice, it is appropriate to define the effective length of $\mathbf{q}$, q, as

$$q^2=2(3-\cos q_x-\cos q_y-\cos q_z)\ , \tag{3.2}$$

and we perform angular averages of $\mathbf{q}$-dependent quantities by averaging over values of $\mathbf{q}$ in the first Brillouin zone, in a spherical shell of mean radius (as given by q) corresponding to that of the vector $(\pi Q/N,0,0)$ and thickness π/N. The value of Q ranges from 1 to approximately $3^{1/2}N$, although only a smaller range is free of finite-size effects. We will, for simplicity of notation, denote quantities averaged in this way by simply dropping the vector symbol from the wave-vector argument $S(q,t)$, and often we will indicate the values of q by the "shell number" Q.

Next we turn to our choices for parameter values. The correlation functions that we are interested in are spatially short ranged. It is therefore not necessary to use extremely large lattice sizes. The results presented were obtained using $N=15$. As in Ref. [39], this proved to be adequate. We checked that finite-size effects do not affect the dynamics in the wave-vector region for which results are presented here ($5<Q<15$; see Sec. IV) by performing a portion of the calculations (with reduced statistics) at $N=25$. Our choice of the ratio σ/h, which fixes the length scale for the problem, is dictated by two concerns. The first is that we wish to be able to study the dependence of the dynamics on wave vector in the main region of interest from the point of view of the static structure factor $S(q)\equiv S(q,t=0)$. Thus, we wish to choose our unit of length so that the main peak in $S(q)$ falls in the

middle part of the range of wave vectors within the first Brillouin zone of the computational lattice. Second, to avoid crystallization at the higher densities studied, we have found that we need N and σ to be incommensurate. Selecting $\sigma/h=4.6$ leaves $q_{\max}$ well away from the zone edge for all densities, near the $Q=8$ shell, and is clearly incommensurate with N. The density range we have investigated includes $n^*=0.5$, $0.75\leq n^*\leq 0.90$, at 0.05 intervals, and $n^*=0.93$. The first of these is well within the dilute liquid region, and was used only to check that limit. As explained in Ref. [39], it is necessary to include the parameter λ in order to represent the actual fluctuations through Gaussian noise. Its precise value is not crucial, since it essentially amounts to a choice of the normalization of the static fluctuations $S(\mathbf{q})$, but it clearly must be small since the density must always be positive. We have taken here $\lambda=0.001$. The remaining parameters K and η are functions of n^* and may be calculated as discussed in Sec. II.

We turn now to the very important question of data collection. We are particularly concerned with ensuring that within statistical error the averages collected be equilibrated, that is, stationary in the time scales studied. We find that, with the data-collection procedure as outlined below, the initial conditions that we use to begin the integration of the equations of the motion are unimportant (except in that they determine to some extent the duration of transient behavior) and we usually take them to be a flat distribution of n equal to its average value n_0 and vanishing currents. We then monitor the current-current correlations as a function of running time t_0. After a relatively short time t_K of order 10, the current correlations reach their equilibrium value as given by the equipartition theorem. It might be tempting to assume that the density correlations have also equilibrated by that time and such an assumption is sometimes made in MD work, but we find that for our system at least this assumption does not hold.

To study the density correlations, we store, for running times $t_0\geq t_K$, where t_0 is the time measured from the initiation of the computation, at a large number of periodic time bins, the products of the form

$$\delta n(\mathbf{x},t_0)\delta n(\mathbf{x}',t_0+t)$$

for all $\mathbf{x},\mathbf{x}'$. We then monitor the spherically averaged spatial Fourier transform $S(q,t,t_0)$ of the quantity

$$S(\mathbf{x},\mathbf{x}',t,t_0)=\langle \delta n(\mathbf{x},t_0)\delta n(\mathbf{x}',t_0+t)\rangle \ , \tag{3.3}$$

where the average is understood to be over a number n_b of time bins separated by an interval Δt. The time range covered by the averaging process is $t_R=n_b\Delta t$. In order for $S(q,t,t_0)$ to be an adequate approximation to the thermodynamic average $S(q,t)$, it is required that it be not only independent of t_0, but also independent of t_R within statistical error. Dependence on the t_0 indicates the presence of a transient. Dependence on t_R indicates that the averaging time is too short for ergodicity to hold. A very important point is that we find that the minimum value of the transient time for density fluctuations is not t_K, but it is of the order of the slowest characteristic decay time t^* in the system. As discussed in Sec. IV, t^* is a strongly increasing function of density, and is much longer than the equilibration time for the kinetic energy. Similarly, it is necessary for the average to include a range t_R of the order of several times t^*. We find that $S(q,t,t_0)$ at higher densities has considerable oscillations over t time ranges smaller than t^*. As one increases the density, an estimate for t^* can be found by extrapolation from the lower densities, since the behavior of t^* with density turns out to obey the Vogel-Fulcher law [22].

Working within these constraints, obtaining statistically reliable results still requires averaging over a large number of time bins, which means very large total running times. In addition, in order to eliminate any possibility of spurious correlations due to a peculiar transient, we have repeated the whole procedure three to five times at each density. The results presented here correspond to a combined total of between 1000 and 3900 bins, depending on the density, at all densities we present results for except $n^*=0.75$, where a total of 600 bins was taken. These very large numbers, much larger than the corresponding numbers in Ref. [39], should be considered as comparable to the "number of runs" in a standard simulation for a nonequilibrium problem such as spinodal decomposition and lead to very good quality data. The cost of obtaining the data rises accordingly, of course: A total of 200 h of Cray 2 and Cray X/MP computer time was required.

We have also verified that the quantity $S(q,t=0)$, calculated following the above procedure and over the time ranges just described, is consistent with the purely static result. To do this, we first calculate the static result: We evaluate numerically, using fast Fourier transforms, the discrete Fourier transform $C(q)$ of (2.3) for a system of the size considered, and we obtain from that result the static result

$$S_s(q)\propto 1/[1-n^*C(q)] \ .$$

To obtain this equation, one must expand the first term in (2.12) to second order in δn. The comparison between $S(q)$ and $S_s(q)$ is shown in Fig. 1. We can see that the

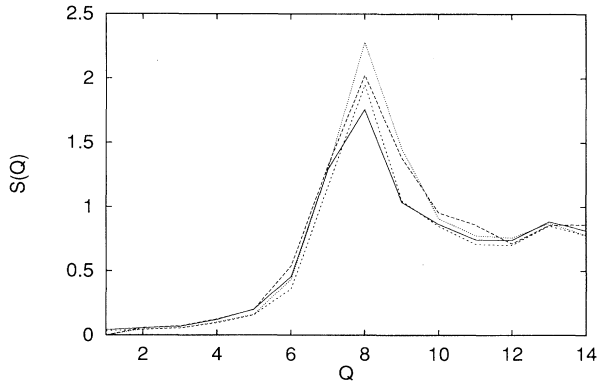

FIG. 1. The static $S_s(Q)$ calculated as explained in the text, compared with the numerical results for $S(Q)=S(Q,0)$. Both quantities are spherical averages plotted vs wave vector as given by the shell number Q defined in the text. The curves shown are for $n^*=0.75$ [$S_s(Q)$, solid line; $S(Q,0)$, long dashes] and for $n^*=0.80$ (static results, short dashes; dynamic results, dots).

two results are in very good agreement at the densities plotted. The PY static values are known to be (see, e.g., Fig. 2 in Ref. [42]) in good agreement with MD results in this density range. Our results then are also in agreement with MD in this limit. At higher densities, the computed result represents a higher degree of order than that calculated from the statics. This is due to the fact that the expansion of the free energy just alluded to is not as well justified at those densities. When averaged over time scales of less than several times t^*, $S(q,0)$ oscillates broadly about its stationary value. Our results for $S(q,0)$ at all densities studied show that we are dealing with a liquidlike state here. If we use a commensurate value of σ, or if we increase n^* to 0.95, we find indications that crystallization begins. We plan to study this crystallization question in future work. The stability of our dynamically obtained results over long computational runs, and their agreement with static results, constitute a very stringent check of the stability of our numerical algorithms.

To analyze our results, it is convenient to introduce the normalized quantity $C(q,t)$ defined as

$$C(q,t)=\frac{S(q,t)}{S(q,t=0)} , \tag{3.4}$$

where, we recall, we are dealing with angularly averaged quantities as explained above with q defined in (3.2). We will then, in Sec. IV, characterize the decay for this quantity for all values of q. By averaging $C(q,t)$ over a large effective number of runs, we are able to obtain results sufficiently smooth to confidently fit functional forms to the data, as Sec. IV demonstrates.

IV. RESULTS AND DISCUSSION

We now turn to the discussion of the normalized dynamic structure factor [see Eq. (3.4)], $C(q,t)$. We have first verified that at low densities ($n^*=0.5$), this quantity decays exponentially at all wave vectors studied. We will consider in what follows only the more interesting range $0.75 \le n^* \le 0.93$. We include in all of our fitting attempts all data up to either the maximum time for which we have data at the particular values of n^* and q under consideration or up to the time where $C(q,t)$ is so small that it fades into the noise. This occurs when $C(q,t)<0.025$ except in some very few cases where the data become noisy at the 0.05 level. As in Ref. [39], the statistical noise seems to have an additive component which causes the relative errors to increase when $C(q,t)$ becomes smaller. We recall that the relation between our time units and Enskog collision time is given by (2.16). The factor relating the two inverse times varies from 1.52 at $n^*=0.75$ to 1.90 at $n^*=0.93$. The relation between our unit of length and σ is the trivial factor of $\sigma/h=4.6$.

We begin by attempting a fit to a stretched exponential form:

$$C(q,t)=e^{-(t/\tau_0)^{\beta}} , \tag{4.1}$$

where the parameters τ_0 and β are functions of n^* and q. This step is motivated in part by the expectation from preliminary inspection of the data that there is a wide region of q and n^* values for which this form is adequate. Indeed, we find that for a considerable part of the data, particularly in the lower density region, this turns out to be a satisfactory fit. Even in the cases where the data are not well fitted by the form of Eq. (4.1), the number $\tau_o(q,n^*)$ still gives a useful figure of merit or overall estimate of the decay time. The results of this fit are in Tables I and II. We have indicated in these tables the cases where the fit to the above form is a good fit to the data and those in which it is actually not the best fit by enclosing the latter cases in parentheses. The quality of the fits can be judged visually and by the χ^2 values that we obtain.

The salient points of the results in Table I are apparent: The characteristic time is at constant density a very strong function of q, and it has a maximum at the wave-vector shells close to where the static structure factor $S(q)$ has its maximum. A less-well-defined secondary maximum at wave vectors close to the second maximum of $S(q)$ can also be discerned. The characteristic time is not, however, of the simple form $\tau_0(q,n^*) \propto \eta S(q)$ as one might guess naively: It is neither proportional to $S(q)$ at constant density (recall η depends on the density only) nor proportional to η at constant q. This indicates, as might be expected, a q-dependent renormalization of the transport characteristic times. This is more marked at higher densities. The stretching parameter β (Table II) remains relatively close to unity, although stretching is evident as one increases the density, particularly at shorter wavelengths. We note that the entries in the Table corresponding to the smaller values of β are in most cases not good fits to the data, as we shall discuss below.

It is apparent from our tabulated results that the slowest overall decay is found, in our spherically averaged results, at the shell number $Q=8$, near the main peak in $S(q)$. We consider then the main decay time τ_0 at that wave vector as representing the slowest transport time at that density t^*. We plot in Fig. 2 this quantity as extracted from Table I as a function of density. We have fitted this quantity to the Vogel-Fulcher [22] law (1.1), which, when the density, rather than the temperature, is the externally controlled variable, takes the form

$$t^*(n^*)=\alpha e^{\gamma/(v-v_c)} , \tag{4.2}$$

TABLE I. The parameter τ_0 of Eq. (4.1) as a function of density as given by n^* and of wave vector as given by shell number Q. The parentheses indicate data sets for which the fit is not satisfactory. These cases are fitted by Eq. (4.3) and Table III.

Q \ n^*	0.75	0.80	0.85	0.90	0.93
6	32	37	38	39	40
7	81	102	133	159	156
8	130	183	424	(1140)	(2271)
9	103	131	208	344	501
10	71	87	112	149	192
11	93	108	125	173	186
12	68	(105)	(118)	(157)	(186)
13	(128)	(197)	(245)	(347)	(430)
14	(134)	(150)	(247)	(221)	(301)

TABLE II. The parameter β of Eq. (4.1) as a function of density as given by n^* and wave vector as given by shell number Q.

Q \ n^*	0.75	0.80	0.85	0.90	0.93
6	0.87	0.84	0.82	0.89	0.84
7	0.95	1.00	0.82	0.93	0.90
8	0.98	0.99	0.84	(0.78)	(0.94)
9	0.96	1.00	1.01	0.94	0.89
10	1.00	0.95	1.04	1.03	0.99
11	0.84	0.91	0.94	0.90	0.93
12	0.83	(0.66)	(0.78)	(0.72)	(0.56)
13	(0.74)	(0.69)	(0.67)	(0.66)	(0.60)
14	(0.69)	(0.77)	(0.47)	(0.54)	(0.32)

where $v \equiv 1/n^*$. As shown in the Figure, we find an excellent fit with a value of v_c corresponding to $n_c^* = 1.23$. This is in excellent agreement with the analysis of MD data of Ref. [28] where the result $n_c^* = 1.21$ was obtained. A three-parameter fit to a power law is also adequate, but the quality of the fit is not quite as good.

We now turn to the decay modes for which the stretched exponential is not a satisfactory fit. We have examined the data very carefully and attempted a large number of fits to different proposed decay forms. We find that the reason for the failure of (4.1) is usually that the decay is a two-step process, or in some cases that the data appear to decay to a finite constant in the time range studied. Accordingly, we have found that the best form that fits this portion of the data is

$$C(q,t) = (1-f)e^{-(t/\tau)^\beta} + fe^{-t/\tau'} , \tag{4.3}$$

where it is understood that the time scales are well separated, $\tau' \gg \tau$. One can also include a stretching exponent in the second decay, but we have found it usually unnecessary and we were leery of multiplying the number of fitting parameters. We note that the form (4.1) is a particular case of (4.3) with $f = 0$ or, alternatively, $\tau \approx \tau'$. It also represents a decay to a constant (quasinonergodic behavior) whenever $\tau' = \infty$, which of course should be understood as meaning that the second decay time is beyond the region fitted. Finally, with f finite, (4.3) yields a region of apparent power-law decay of the von Schweidler form when $\tau \ll t \ll \tau'$ and the time scales are widely separated. We find that this very general form fits well (again, as measured by the appropriate reduced χ^2 values and visually) all cases where, as indicated by the parentheses in Tables I and II, the single decay fit was not satisfactory. The parameters τ, τ', and f are given in Table III. The parameter β turned out to be very close to unity in all of these cases. In Figs. 3 and 4 we show a wide selection of our results and the corresponding best fits, according to the parameters in Tables I–III. For every density we have two figures, which display the decay of $C(q,t)$ at that density for a sampling of wave-vector values. The values shown are $Q = 6$, 8, 10, 12, 13, and 14. These include all Q values where the decay is not of the form (4.1). Values skipped have been omitted to avoid excessive clutter. Keeping in mind the figures and the three tables, we see very clear trends. First, as one increases the density, nonexponential behavior crops out first at relatively larger wave vectors, that is, shorter distances, which is physically sensible and was observed also in Ref. [39]. Specifically, this behavior appears first at values beyond the main peak in the structure factor, in the region of the second peak. As the density increases further, the beginning of the same phenomenon is observed at smaller wave vectors at or near the main peak in $S(q)$. This phenomenon appears to be related to the q dependence of β found in mode-coupling calculations [47]. The characteristic times increase strongly with density, and so does their relative separation. They are also strongly q dependent. On the other hand, f appears to depend rather weakly on n^* but more strongly on q, and its q dependence appears also to correlate with that of the

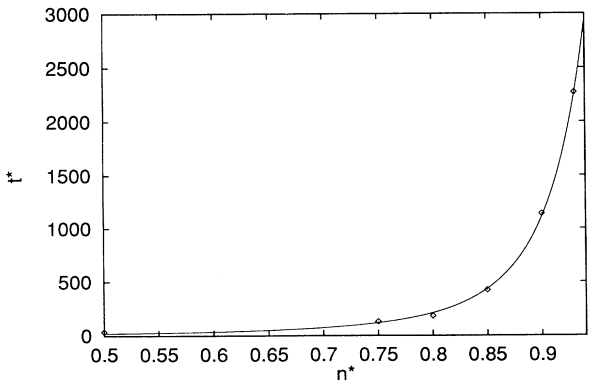

FIG. 2. The characteristic decay time t^* plotted as a function of density n^*. The data are fitted to a Volger-Fulcher form, as explained in the text.

TABLE III. The parameters τ, τ', and f of Eq. (4.3) for the appropriate range of n^* and Q values (see text and Tables I and II). The values of τ' indicated by infinity must be interpreted as being beyond the time window fitted. The three daggered values of τ' indicate cases where an exponent β' different from unity was required. In these cases β was set to unity, so the number of parameters was the same, but in the other cases the unrestricted β remained close to unity.

Q	Parameter \ n^*	0.75	0.80	0.85	0.90	0.93
8	τ				561	942
	τ'				3115†	4231†
	f				0.34	0.45
12	τ		83	98	131	149
	τ'		∞	∞	∞	∞
	f		0.08	0.07	0.07	0.09
13	τ	51	64	104	107	171
	τ'	239	397	615	761	1210
	f	0.55	0.56	0.44	0.53	0.42
14	τ	94	112	135	159	219
	τ'	702†	∞	∞	∞	∞
	f	0.13	0.14	0.18	0.16	0.14

statics. From the point of view of (4.3), it appears that the lower-density stretched exponential form (4.1) should be viewed as arising from a confluence of the time scales, rather than from the vanishing of f.

We also monitor the value of the mean-field free energy during the computation. We find that the system fluctuates around a liquidlike state minimum. Thus, our simulations establish that the first three or four orders of magnitude in the growth of the relaxation time in the hard-sphere system arise from the effects of nonlinearities associated with the realistic free energy used.

It is very instructive to discuss our results in connection with MD work, with mode-coupling theoretical work on glassy systems, and with experiment. Some caution is required, however, since it must be kept in mind that we are dealing here with relatively low densities: The degree of supercooling that our choices of N and σ achieve is limited in comparison with what can be done experimentally. We have not used other procedures, such as mixing spheres of two different sizes, which might allow further increases in the density. There are a variety of decay regimes and forms reported in the literature for glassy systems. A scenario in favor of which some consensus has gathered [17] is described in the In-

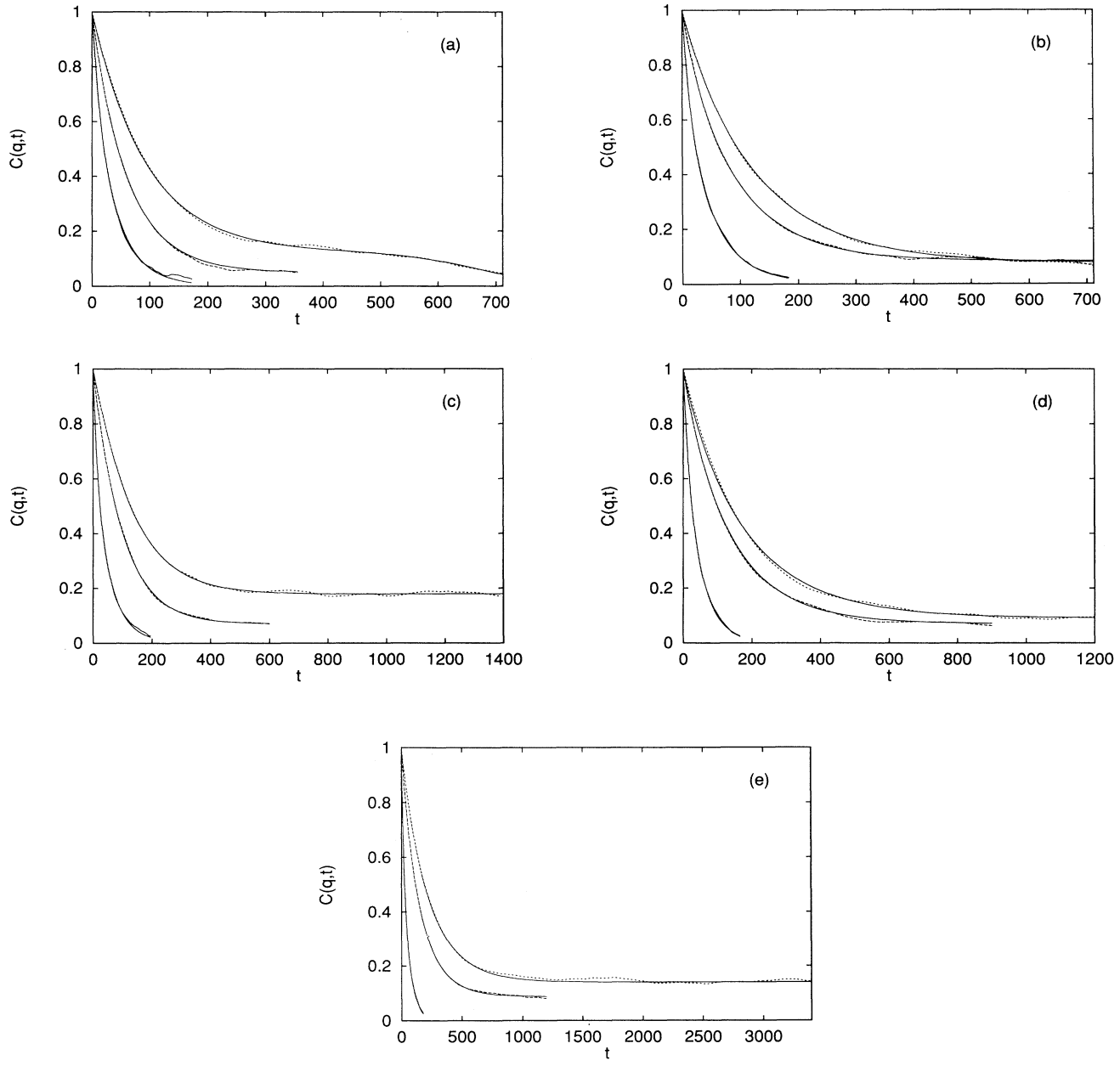

FIG. 3. The normalized correlation function $C(q,t)$ plotted vs t for $Q=14$ (top curve), 12, and 6 (bottom curve). The data and the best functional fits smooth (solid curves) as explained in the text are shown for $n^*=$ (a) 0.75, (b) 0.80, (c) 0.85, (d) 0.90, and (e) 0.93.

troduction. We believe that our results at higher densities and shorter distances, in the region where the full form (4.3) is obeyed might be interpreted within the above scheme as representing a first decay which combines phonon and β relaxation, leading eventually to the second decay, which might then be identified with α relaxation. In some cases only the quasinonergodic regime is reached in our computations. The von Schweidler regime can arise, as explained above, as a precursor of the second decay. The phonon-assisted decay does not appear as a separate regime in our data, which is possibly due to the coarse-graining nature of Langevin dynamics with respect to microscopic times. We have verified that an inverse power law does not fit the earlier portion of our data as well as a stretched exponential form.

We have already mentioned the agreement of our results for t^* and $S(q)$ with the MD results of Refs. [28] and [42], respectively. Comparison with MD work on glass dynamics is complicated by the fact that such MD results are for different systems, such as binary soft-sphere mixtures (see, e.g., Refs. [30] and [32]) or Coulombic systems [31]. Obviously, detailed comparisons will have to await further work. However, as results for different MD systems are qualitatively consistent with each other, a qualitative comparison with our results is possible. Although comparison of MD and Langevin

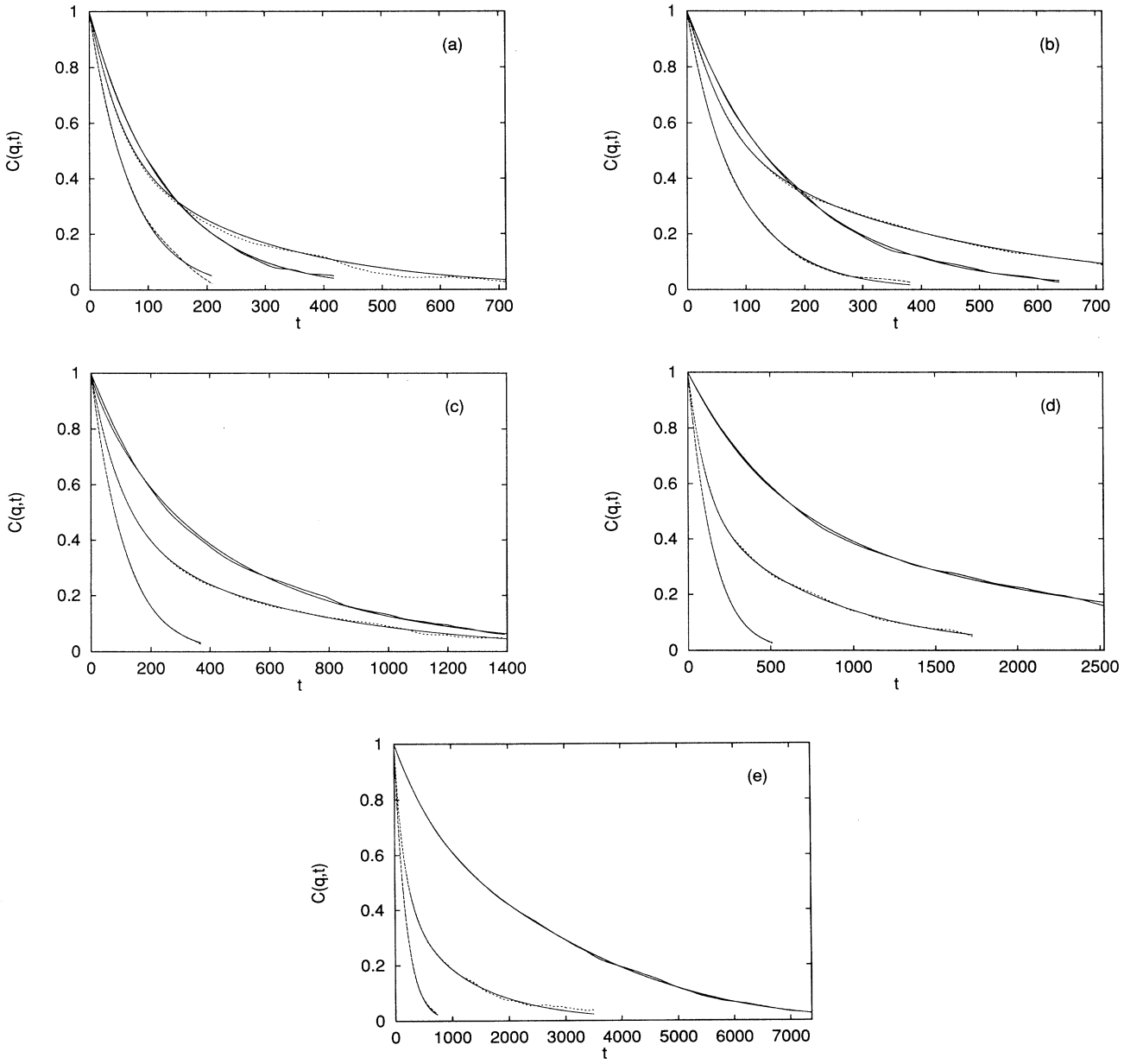

FIG. 4. As in the previous figure but for $Q=8$ (top curve at $t=100$), 13, and 10 (bottom curve).

time scales is in general a vexing problem, for our purposes here it might be adequate to simply assign to our phonon-based time unit a value of order 0.1 ps. We then find that the results of Ref. [30] correspond to a shorter time range than our higher-density results, while those of Refs. [32] and [31] are comparable. Neither Ref. [32], which covers higher densities than ours, nor Ref. [31], follow $C(q,t)$ until it decays to zero or to a small value, as we do, and they assume that their systems have reached equilibrium when the kinetic energy equilibrates, an assumption which we checked and found, for our dynamics, erroneous. We do not know if this is also the case for MD. Despite all of these caveats, our results are consistent with those of both Refs. [32] and [31]. They observe first a glitch at very early times, which they attribute to phonons, and then two relaxation modes separated by a slow region, which they identify with β and α relaxations. They do not attempt to quantitatively characterize the β regime by either a power law or an exponential, but they do obtain an exponential form (stretched at higher densities) for the second decay. As stated above, our data do not show any early time glitch, which could be due either to Langevin coarse graining, or to the glitch being an artifact of poor system equilibration. Except for this, our results are consistent with MD in that a naive extrapolation of our results to higher densities would predict that the time scales τ and τ' in (4.3) become more separated, and possibly larger values of f appear. We have verified that the MD data of Ref. [31] can in fact be fit to the form (4.3) with appropriate parameter values. Thus we conclude that our results are consistent with MC as well as MD.

ACKNOWLEDGMENTS

We are indebted to G. F. Mazenko for many, very useful discussions about this problem. L.M.L. was supported in part by the Department of Education. C.D. thanks the School of Physics at the University of Minnesota and the Minnesota Supercomputer Institute for support and hospitality and S. Ramaswamy for useful discussions. This work was supported in part by grants from the Cray Research Corporation and the Minnesota Supercomputer Institute.

[1] J. Jackle, Rep. Prog. Phys. **49**, 171 (1986).
[2] C. A. Angell, J. Phys. Chem. Solids **49**, 863 (1988).
[3] For reviews of mode-coupling theories, see W. Götze and L. Sjogren, in *Dyanamics of Disordred Materials,* edited by D. Richter, A. J. Dianoux, W. Petry, and J. Teixeira (Springer, Berlin, 1989); B. Kim and G. F. Mazenko, Adv. Chem. Phys. **78**, 129 (1990).
[4] E. Leutheusser, Phys. Rev. A **29**, 863 (1984).
[5] U. Bengtzelius, W. Götze, and A. Sjolander, J. Phys. C **17**, 5915 (1984).
[6] W. G. Götze, Z. Phys. **60**, 195 (1985).
[7] W. Götze and L. Sjogren, Z. Phys. B **65**, 415 (1987); J. Phys. C **21**, 3407 (1988); J. Phys. Condens. Matter **1**, 4183 (1989).
[8] T. R. Kirkpatrick, Phys. Rev. A **31**, 939 (1985).
[9] S. P. Das and G. F. Mazenko, Phys. Rev. A **34**, 2265 (1986).
[10] S. P. Das, Phys. Rev. A **36**, 211 (1987).
[11] N. Tao, G. Li, and H. Z. Cummins, Phys. Rev. Lett. **60**, 1334 (1990).
[12] See, for example, B. Frick, B. Farago, and D. Richter, Phys. Rev. Lett. **64**, 2921 (1990); W. Petry *et al.*, Z. Phys. B **83**, 175 (1990).
[13] G. Williams and D. C. Watts, Trans. Faraday Soc. **66**, 80 (1970).
[14] P. K. Dixon, L. Wy, S. R. Nagle, B. D. Williams, and J. P. Carini, Phys. Rev. Lett. **66**, 960 (1991).
[15] I. C. Halalay and K. A. Nelson, Phys. Rev. Lett. **69**, 636 (1992).
[16] J. Colmenero, A. Alegria, A. Arbe, and B. Frick, Phys. Rev. Lett. **69**, 478 (1992). See also other neutron work cited above.
[17] B. Kim and G. F. Mazenko, Phys. Rev. A **45**, 2393 (1992).
[18] T. R. Kirkpatrick, D. Thirumalai, and P. G. Wolynes, Phys. Rev. A **40**, 2 (1989).
[19] D. L. Stein and R. G. Palmer, Phys. Rev. B **38**, 12 035 (1988).
[20] J. P. Sethna, Europhys. Lett. **6**, 529 (1989).
[21] J. P. Sethna, J. D. Shore, and M. Huang, Phys. Rev. B **44**, 4943 (1991).
[22] H. Vogel, Z. Phys. **22**, 645 (1921); G. S. Fulcher, J. Am. Ceram. Soc. **8**, 339 (1925).
[23] Here, and elsewhere in the paper, the term "thermodynamic equilibrium" means equilibrium over a restricted phase space that excludes the crystalline state.
[24] W. Kauzmann, Chem. Rev. **48**, 219 (1948).
[25] C. Dasgupta, A. V. Indrani, S. Ramaswamy, and M. K. Phani, Europhys. Lett. **15**, 307 (1991).
[26] R. M. Ernst, S. R. Nagel, and G. S. Grest, Phys. Rev. B **43**, 8070 (1991).
[27] E. W. Fisher, E. Donth, and W. Stephen, Phys. Rev. Lett. **68**, 2344 (1992).
[28] L. V. Woodcock and C. A. Angell, Phys. Rev. Lett. **47**, 1129 (1981).
[29] J. J. Ullo and S. Yip, Phys. Rev. Lett. **54**, 1509 (1985); Phys. Rev. A **39**, 5877 (1989).
[30] J. J. Ullo and S. Yip, Chem. Phys. **149**, 221 (1990).
[31] G. F. Signorini, J.-L. Barrat, and M. W. Klein, J. Chem. Phys. **92**, 1294 (1990).
[32] J.-L. Barrat, J.-N. Roux, and J.-P. Hansen, Chem. Phys. **149**, 197 (1990).
[33] F. Mezei, W. Knaak, and B. Farago, Phys. Rev. Lett. **58**, 571 (1987); Phys. Scr. **19**, 363 (1987).
[34] NFH as formulated here was first used in the study of fluids by O. T. Valls and G. F. Mazenko, Phys. Rev. B **44**, 2596 (1991). For a review of the formalism, see B. Kim and G. F. Mazenko, J. Stat. Phys. **64**, 631 (1991).
[35] T. V. Ramakrishnan and M. Yussouff, Phys. Rev. B **19**, 2275 (1979); D. W. Oxtoby, in *Liquids, Freezing and the Glass Transition,* Lecture Notes of the Les Houches Summer School, 1989, edited by J.-P. Hansen, D. Levesque, and J. Zinn-Justin (Elsevier, New York, 1990).
[36] C. Dasgupta, Europhys. Lett. **20**, 131 (1992); C. Dasgupta and S. Ramaswamy, Physica A **186**, 314 (1992).
[37] J. P. Hansen and I. R. McDonald, *Theory of Simple Liquids* (Academic, London, 1986).

[38] O. T. Valls and G. F. Mazenko, Phys. Rev. A **44**, 2596 (1991).
[39] O. T. Valls and G. F. Mazenko, Phys. Rev. A **46**, 7756 (1992).
[40] J. L. Barrat, W. Götze, and A. Latz, J. Phys. Condens. Matter. **1**, 7163 (1989).
[41] O. T. Valls and G. F. Mazenko, Phys. Rev. B **38**, 11 643 (1988).
[42] W. E. Alley, B. J. Alder, and S. Yip, Phys. Rev. A **27**, 3174 (1981).
[43] J. P. Boon and S. Yip, *Molecular Hydrodynamics* (McGraw-Hill, New York, 1990), Eq. 2.4.40.
[44] J. E. Farrell and O. T. Valls, Phys. Rev. B **40**, 7027 (1989).
[45] We have set the combination $(\zeta+\eta/3)$, where ζ is the bare bulk viscosity, to zero, mainly for reasons of simplicity in generating the noise correlations.
[46] J. P. Boon and S. Yip, *Molecular Hydrodynamics,* Ref. [43], Eq. 6.7.21.
[47] M. Fuchs, I. Hofacker, and A. Latz, Phys. Rev. A **45**, 898 (1992).